Archives of Mechanics • Archiwum Mechaniki Stosowanej • 28, 5–6, pp. 827–836, Warszawa 1976

Initial experimental results for liquefaction shock waves in organic fluids

G. DETTLEFF, P. A. THOMPSON and G. E. A. MEIER (GÖTTINGEN)

UNDER certain conditions it is possible to produce shock waves for which the upstream state is vapour and the downstream state is liquid: that is, the shock front is also a surface of phase discontinuity. We have studied the behaviour of condensation waves of this type in shock tube experiments. The shock tube is heated to steady-state temperatures up to 150°C. We report here on the nature of phase-transition (shock) front, the fluid properties upstream and downstream of the shock, and the agreement between the experiments and shock theory.

Praca dotyczy własności fal uderzeniowych, powstających w warunkach, gdy w rozpatrywanym obszarze przed przejściem fali występuje para, a po przejściu fali — ciecz. Własności tego rodzaju fal kondensacyjnych badano doświadczalnie za pomocą rury uderzeniowej. Układ eksperymentalny umożliwiał otrzymanie temperatur w rurze uderzeniowej do 150°C. Przedstawione rezultaty dotyczą własności frontu fali (z przejściem fazowym) oraz własności płynu przed i po przejściu fali uderzeniowej. Wyniki doświadczalne porównano z przewidywaniem teorii fal uderzeniowych.

Работа касается свойств ударных волн, возникающих в условиях, когда в рассматриваемой области перед переходом волны выступает пар, а после перехода волны — жидкость. Свойства этого рода конденсационных волн исследованы экспериментально при помощи ударной трубы. Экспериментальная система дает возможность получения температур в ударной трубе до 150°C. Представленные результаты касаются свойств фронта волны (с фазовым переходом), а также свойства жидкости перед и после перехода ударной волны. Экспериментальные результаты сравнены с предсказаниями теории ударных волн.

1. Introduction

THE INTERPLAY between condensation phenomena and compressible flow has been studied for many years. The early work of STODOLA (1927) on the condensation of steam in supersonic steam-turbine nozzles has been followed by many related investigations in high-speed flow. The unifying feature of these investigations is the production of a super-saturated vapour state leading to condensation by means of adiabatic expansion. A recent summary of flows of this kind is given by WEGENER (1969).

It can be said that the gasdynamic phenomena in expansion flows with condensation are well-known (though not necessarily perfectly understood). There is, however, a quite different class of flows in which condensation results from compression rather than expansion. Thus far, such flows have not been widely investigated. This paper deals with one aspect, the sudden condensation of a vapour by means of a shock wave.

It is necessary to say something about the terminology applied to more or less abrupt wave-like processes in flows with condensation. In the traditional expansion flows there are two main kinds of processes which may loosely be described as "condensation discon-

tinuities". In the first kind, dropwise condensation of a rapidly flowing (usually supersonic) supersaturated vapour takes place over a relatively short distance, with a typical length scale of 10^{-2} m (depending strongly on canal geometry). In the absence of an accepted compact description for a process of this kind, it may be called "abrupt condensation of a flowing supersaturated vapour". In the second kind of process a conventional shock wave can, under certain conditions, result from the heating of the gas by the released latent heat of condensation. Depending partly on geometry, there may be a more or less complicated pattern of shock waves and condensation zones. An individual shock wave in this second case has been called a "condensation shock wave" and has a typical length scale of 10^{-7} m. Unfortunately, the term "condensation shock" has also been sometimes applied to the first kind of process discussed above (THOMPSON 1972); another difficulty is that the term does not appear to be descriptive — the effect of the shock wave itself is actually to produce evaporation. Perhaps "condensation-induced shock" would be a better term.

For the compression shock waves with associated condensation discussed in this paper there is in any case no well-established terminology. In its "pure" or essential form this shock has a vapour upstream state and a liquid downstream state, the transition from vapour to liquid being effected by the compression process in the shock wave. This kind of shock wave is thus entirely distinct from the traditional expansion-flow phenomena described above. The problem is to find a clear and descriptive name. The term *condensation shock wave* is simple and has been used by THOMPSON and SULLIVAN, but has the disadvantage of being possibly confused with the expansion-flow phenomenon. The alternative term *liquefaction shock wave*, relatively clear and possibly more attractive from the etymological viewpoint, will be used in this paper and in future papers dealing with this phenomenon.

A vapour can be condensed by the shock compression process only if the condensate can store or "contain" the latent heat for the phase change without re-evaporating. This will be the case only if the heat capacity of the substance (as represented by some standard heat capacity) is sufficiently large (THOMPSON and SULLIVAN 1975). This restricts the substances for which a liquefaction shock is possible to those with a large number of internal molecular degrees of freedom. It is thus convenient to associate the traditional expansion-flow condensation phenomena with simple molecules, such as those of water, and to associate the liquefaction shock phenomena discussed in this paper with complex molecules, such as those of normal octane.

2. Theoretical sketch

The description of a liquefaction shock in terms of classical shock-discontinuity theory has been given by THOMPSON and SULLIVAN. We shall here summarize the essential results.

A liquefaction shock for which the transition from an upstream vapor state to a downstream liquid state is complete, i.e., the upstream state is "fully dry" and the downstream state is "fully wet" may be called *complete*. The basic minimal version of a complete liquefaction shock has a saturated vapour upstream state (1) and a saturated

liquid downstream state (2). It is convenient to discuss the theory in terms of this basic discontinuity.

Isentropic compression is a limiting case for the compression process in a shock wave. Condensation by a shock wave will not be possible unless isentropic compression leads to condensation. Fluids having this property are said to be retrograde. It is convenient to characterize the fluid behaviour in this respect by a characteristic heat capacity $\tilde{c}_v$, namely the ideal-gas heat capacity c_v^0 evaluated at the critical temperature, normalized by the gas constant R

$$\tilde{c}_v = c_v^0(T_c)/R. \tag{2.1}$$

The minimum value of $\tilde{c}_v$ for retrograde behavior is $\tilde{c}_v \approx 11.2$. Fluids (such as water or nitrogen) with a smaller value of $\tilde{c}_v$ show regular condensation behaviour; fluids (such as benzene or *n*-decane) with a larger value of $\tilde{c}_v$ show retrograde behaviour. The possible cases are shown in Fig. 1.

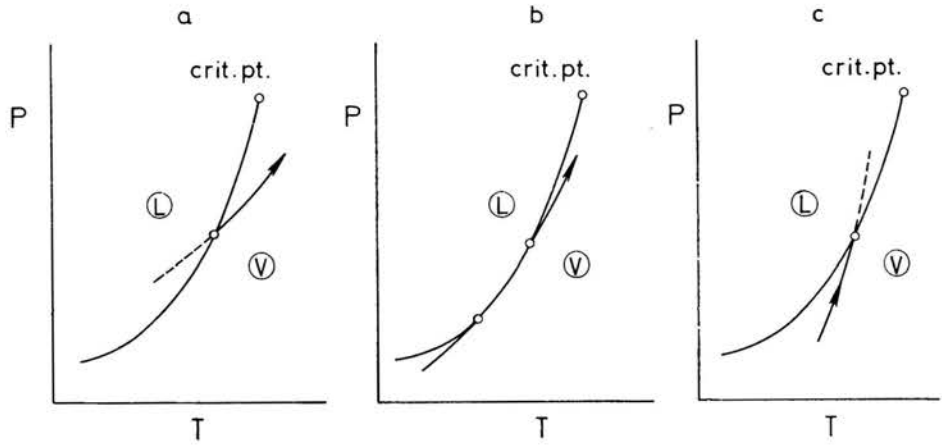

FIG. 1. Saturation curves and compression isentropes for the three possible cases of regular, isentropic and retrograde fluid behaviour. a) Regular fluid in which isentropic compression of the vapour superheats the vapour. b) Isentropic fluid in which, for the limiting isentrope, isentropic compression produces neither, superheat nor condensation. c) Retrograde fluid in which isentropic compression of the vapour leads to condensation.

In the liquefaction shock there is an increase in entropy across the shock. This means that the minimum heat capacity $\tilde{c}_v$ permitting complete condensation will be considerably greater than the limiting value for retrograde behaviour. Detailed calculations show that this minimum heat capacity is $\tilde{c}_v \approx 24.1$, which corresponds roughly to the value for normal hexane. Depending on the technique used, a practical laboratory demonstration of a liquefaction shock might require a value $\tilde{c}_v \geqslant 40$. We thus have the following values for the characteristic heat capacity:

retrograde behaviour	$\tilde{c}_v > 11.2$,
theoretical limit for liquefaction shock	$\tilde{c}_v = 24.1$,
practical experiments with liquefaction shock	$\tilde{c}_v > 40$.

The shock adiabats for a liquefaction shock are shown in Fig. 2. For any given downstream state (2) on the saturated liquid boundary, there are two possible upstream states (1) on the saturated vapour boundary.

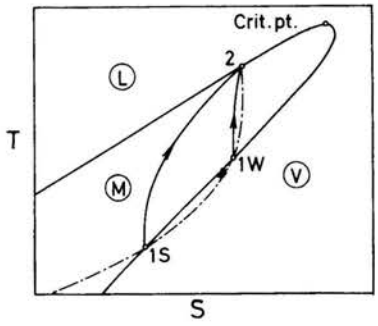

FIG. 2. Shock adiabats drawn in the temperature-entropy plane for the weak (W) and strong (S) solutions leading to a common downstream state 2. The conventional forward adiabats are shown, solid and the inverse adiabat is dashed. (Redrawn from THOMPSON and SULLIVAN).

The calculation of state changes from the Rankine-Hugoniot equation and the usual shock conditions is straightforward and requires only an adequate equation of state. The most striking feature of the calculation is that the downstream (liquid) densities are large. This means, for example, that the fluid downstream of the shock moves quite slowly with respect to the shockfront.

3. Experimental objectives

Our experimental program includes in part the following objectives: a) to demonstrate the basic phenomenon of condensation across a compression shock wave, b) to demonstrate the existence of a complete liquefaction shock, c) to compare the dynamic states found in experiments with those predicted by equilibrium thermodynamics, d) to observe any odd or interesting physical phenomena which might arise.

There are several physical arrangements which could conceivably be used to produce a liquefaction shock wave, including (among others) the following: a) a supersonic steady-flow vapour tunnel, b) a shock tube arranged to produce a direct liquefaction shock running into the organic test gas, c) a shock tube arranged to produce the liquefaction shock as the reflected shock at the closed end of the test section. The first technique (a) involves difficulties with liquid → vapour phase changes in attempting to produce a near-saturation vapour which moves with supersonic velocity in a retrograde fluid. The second technique (b) is complicated by the high density of the downstream liquid state, which requires that the driver/test contact surface travel a very short distance ($\sim$ 1 cm) behind the liquefaction shock. For the experiments described here, we have mostly used the reflected-shock technique (c).

4. Experimental apparatus and procedure

The shock tube used in the experiments is shown in Fig. 3. Special features include electrical heating of the entire insulated tube, permitting temperatures up to 160 °C, and provision for introducing the test fluid in the liquid phase.

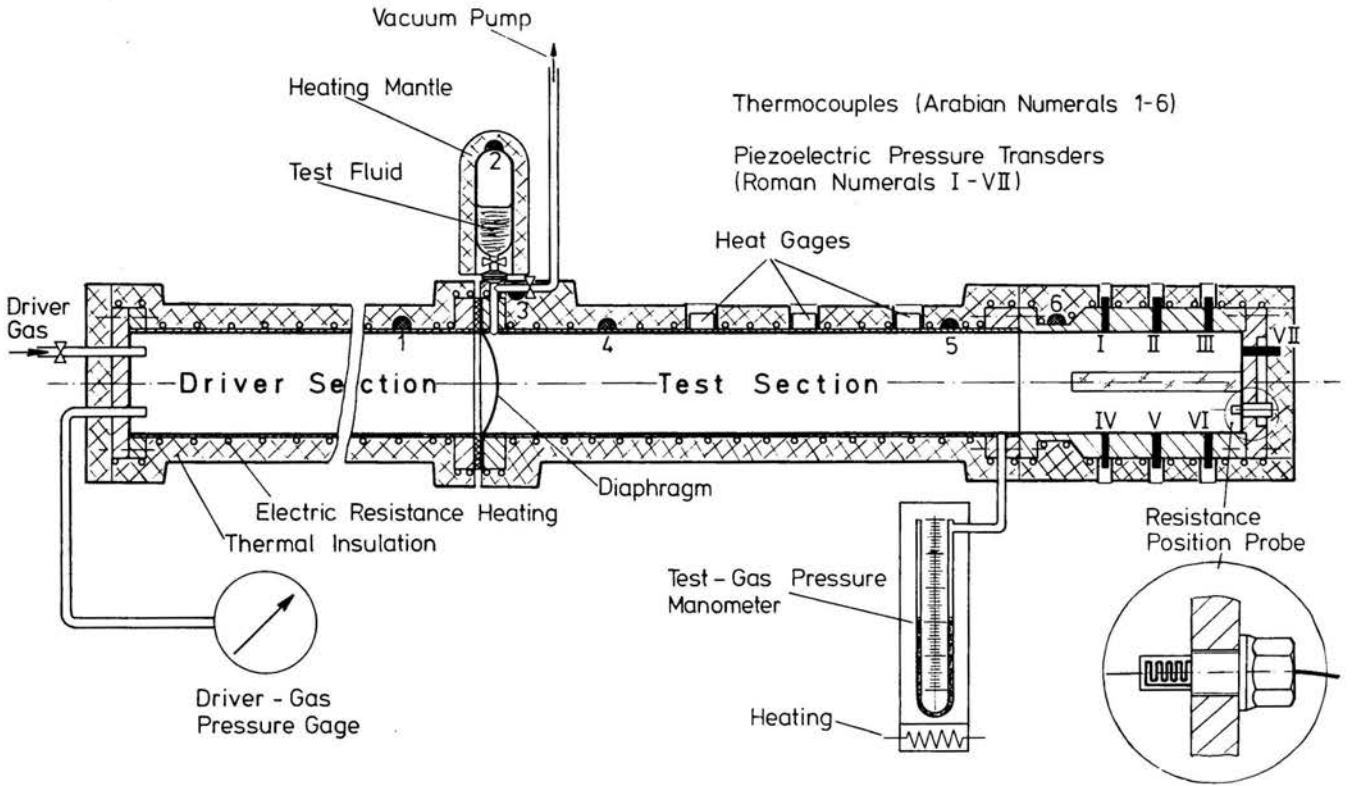

FIG. 3. Shock tube schematic, showing the method of introducing the test fluid and location of instrumentation. Thermocouples are indicated by the Arabian numerals (1–6) and piezoelectric pressure transducers by the Roman numerals (I–VII). Not drawn to scale.

It is intended that the liquefaction shock appear as the reflection of the test-gas shock initiated by the diaphragm burst. This shock, labelled R in the wave diagram of Fig. 4, travels away from the closed end of the test section. Because the downstream state (2) has a high density, the shock R travels very slowly away from the wall, with a velocity in the order of 10 m/s. Most of the interesting condensation (and later evaporation) phenomena are thus concentrated within a few centimeters of the closed end of the test section. This part of the shock tube is in fact a structurally separable *observation section*, fitted with a narrow window on each side, and most of the instrumentation is concentrated there.

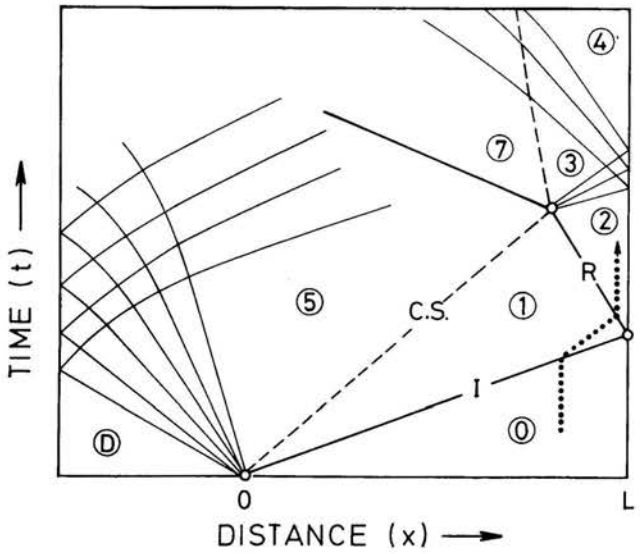

FIG. 4. Ideal wave diagram for the test-fluid flow, with Arabian numerals designating the various test-fluid states. Other designations are I — incident shock, R — reflected (liquefaction) shock, C. S. — contact surface, D — driver gas initial state. Not drawn to scale.

The diaphragms used have been mainly Dupont Capton polyamide with thicknesses between 125 and 150 μ. The burst takes place when a sufficient pressure is reached in the nitrogen driver gas, introduced from a gas bottle, without any artificial means for rupture initiation.

In a normal cycle of operation, the tube is heated to a steady-state temperature T_0, corresponding to the desired initial temperature for state (0) in Fig. 4. The diaphragm is then mounted and the test section evacuated. The test fluid is metered into a sample holder which is then mounted on top of the tube, heated to approximately temperature T_0, and allowed to flow into the test section where it evaporates. After recording the initial temperature, pressure, mass of test fluid, and so on, diaphragm burst is initiated by pressurizing the test section. The pressure signals from the piezoelectric transducers along with other measurement signals are displayed and photographed on a multichannel oscilloscope.

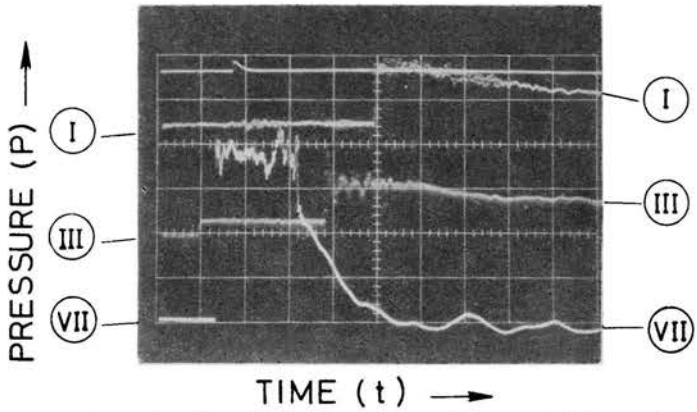

FIG. 5. Pressure history from the piezoelectric transducers. Run No. 31/V4. Vertical pressure scale: 3 bars/div (I, VII) and 5 bars/div (III). Time scale: 0.5 ms/div. Test fluid: Flutec PP3, $m_0 = 40.0$ g. Temperature $t_0 = 88°C$. Driver pressure $P_D = 4.5$ bars. The uppermost trace shows the signal from a photodiode, marking the time at which a flashtube used for the photography was fired.

In order to record the position of the reflected liquefaction shock, a resistance position probe was constructed and driven by a hot-wire manometer supply. The probe consists of thin vapour-deposited conductive strips which are progressively covered (from left to right) by the relatively hot fluid behind the reflected shock.

The test fluid used in the experiments was "Flutec PP3", a proprietary fully-fluorinated dimethylcyclohexane purchased from the Imperial Smelting Company. The essential thermodynamic parameters(*) characterizing this fluid are: critical pressure $P_c = 18.81$ bar, critical temperature $T_c = 514.65$ K, critical volume $v_c = 1.520$ cm^3/g, Riedel parameter $\alpha_c = 8.11$, characteristic heat capacity $\tilde{c}_v = 53.88$, molecular weight $\tilde{M} = 400.064$. The thermodynamic properties for this fluid were determined from an equation-of-state similar to the one discussed by Thompson and Sullivan, and checked against values obtained from the Imperial Smelting tables.

5. Experimental results

The essential experimental data are the following: initial temperature, pressure, and specific volume in the test gas; the pressure histories $P(t)$ from the piezoelectric transducers; the position signal $I(t)$ from the resistance probe; photographs obtained by direct photography through the windows in the observation section. These data, in conjunction with an equation-of-state description of the test fluid and the equations of shock dynamics, provide a redundant description of the test-fluid states (0, 1, 2).

In most of the experiments the initial test-fluid conditions, the driver-gas pressure P_D, and diaphragm thickness were chosen such that the initial state (0) was well superheated and the first shocked state (1) was close-to-saturated vapour, that is, either slightly

(*) Tables of thermodynamic properties for Flutec PP3, Imperial Smelting Corp. Ltd., Avonmouth, Bristol 1970.

superheated or slightly wet. In some of the photographs, however, a thin fog of fine liquid droplets (estimated diameter $\sim 10^{-7}$ m) was observed even when the shocked state (1) was nominally dry. In the later phases of the test-gas flow (near the contact surface) this is probably a result of mixing with the driver gas, which has been strongly cooled through adiabatic expansion. In addition, some fog may result from the condensation of a small quantity of fluid on the shock-tube wall, which is invariably colder than the saturation temperature t_{2S} at the test pressure P_2.

The test conditions were further chosen in most cases such that the shocked state (2) behind the reflected liquefaction shock was close-to-saturated liquid or compressed liquid. We now describe the extent to which this state was achieved in terms of the experimental results.

A representative pressure trace is shown in Fig. 5. The arrival of the incident shock I at the end wall is shown by the large jump (about 12 bars) in the signal from transducer VII. The following roughly level plateau in this signal, lasting about 1 ms, corresponds approximately to the duration of the liquefaction-shock phenomenon. During the later half of this plateau period, however, photographic observations indicate that there is considerable mixing of small quantities (by mass) of the driver gas with test fluid: this seems to be confirmed by the increasing irregularity of the signal. The sudden drop in pressure at the end of the plateau period marks the arrival of the effective contact surface at the reflected shock R, that is, the inflowing test fluid has been exhausted, having been almost completely converted to liquid. Because the density of the driver gas is smaller than that of the shocked test gas (1), the momentum flux ϱu^2 into the shock is dramatically reduced and a rarefaction wave travelling toward the end wall is initiated: the reflection of this rarefaction from the fixed end wall is marked by the abrupt termination of the plateau period. A consequence of the rarefaction is that re-evaporation of the test fluid is begun. (We should remark here that the driver section of the shock tube has been made sufficiently long so that the arrival of the driver-gas rarefaction from the other end of the shock tube arrives later and plays no role in the above.)

Assuming that all of the test gas were converted to liquid, the final (maximum) length of liquid L_L in the observation section is fixed by the ratio of the liquid specific volume v_2 to the test-gas specific volume v_0. For typical experiments this gives $L_L \approx (v_2/v_0)L \approx$ $\approx$ (0.8/300) 240 $\approx$ 0.6 cm.

The (equilibrium) state (1) is fully fixed by the initial state (0) and the strength of the incident shock I, through the Rankine-Hugoniot equation. The state (2) is then fully fixed by the fixed-wall condition $u_2 = 0$ with the Rankine-Hugoniot equation. Thus, the final state (2) can be found from the initial state (0) and some measure of the incident-shock strength, which we have taken to be the shock velocity V_I, found from the pressure signals from transducers I and III. The input data for the calculation are the temperature t_0, specific volume v_0, and shock velocity V_I. The results of the calculation and a comparison with experimental data are shown in Table 1.

The calculations agree well with the measured values for the pressures P_0, P_1, and P_2, lending credibility to the final calculated volume $v_2 = 0.80$ cm^3/g, well within the compressed-liquid region: at the calculated temperature t_2, the saturation pressure is about 9.5 bars. For comparison, a perfect-gas model yields for the same initial con-

Table 1. Results from run No. 83/V1

Property		Measured	Calculated
t_0	°C	88*	
v_0	cm³/g	300*	
P_0	bar	0.24	0.25
c_0	m/s		85.7
V_I	m/s	234*	
t_1	°C		120
v_1	cm³/g		40
P_1	bar	1.80	1.85
u_1	m/s		204
t_2	°C		201
v_2	cm³/g		0.80
P_2	bar	12.3	12.5

* Input data for calculated results

ditions (0) the values $P_2 = 12.3$ bars and $v_2 = 7.10$ cm³/g: however, this model is physically inappropriate (condensation is photographically and otherwise observed) and the agreement with the measured value of P_2 is fortuitous, since the perfect-gas and real-gas adiabats are not congruent.

There are three other kinds of observations which tend to support the conclusion that the end state (2) is liquid, namely position-probe measurements, photography, and visual observation. The records from the position probe indicate a reflected shock velocity in the range 6–20 m/s, these very low velocities corresponding to what one would predict for a liquid state behind the liquid shock. Th eposition probe technique is, however, still undeveloped at this writing and the velocity values are not reliable.

Conventional photographs of the flow in the test section show several interesting results. Quite striking is the appearance of an (apparently) bifurcated foot shock structure in the reflected shock, a structure often observed in conventional shock waves reflected from the closed end of a shock tube, as discussed for example by DAVIES and WILSON (1967). In our case the upstream-pointing foot seems to extend very far ahead of the liquefaction shock itself and is filled with an opaque dense fog: thus, pictures taken at a 90° angle to the shock-tube axis show only the profile of the leading edge of this foot. In a typical case, this leading edge may be 20 mm away from the fixed shock tube end wall while the central liquefaction shock is estimated to be only about 4 mm away from the end wall. In photographs taken obliquely, i.e., looking towards the end wall, however, one sees the opaque foot and an essentially transparent central region, indicating that the fluid behind the reflected shock is a liquid, or at least a single-phase fluid.

Finally, liquid condensation on the end wall of the shock tube can be observed by the eye when the observation section is brightly illuminated by a steady light source. It seems that many compression — rarefaction cycles produce a corresponding liquefaction — evaporation near the end wall. After twenty or more cycles (lasting roughly 0.2 s) the test fluid is confined to a small region and is nearly at rest in the observation section.

This terminal state of liquefaction, partly thermally-induced (compare the work of SMITH 1973, who observed small quantities of thermal condensate with CCl_4), is presumably what is seen. It is followed by a slow evaporation (lasting roughly 1 s) associated with diffusion of the test-fluid vapour into the driver gas.

The experimental techniques discussed above, the position probe and photographic observation, have not yet reached a satisfactory stage of development.

6. Conclusions

The evidence suggests that condensation across the liquefaction shock leads to a liquid downstream state. However, the absence of adequate experimental techniques for direct observation of the liquefaction shock, i.e., of the phase discontinuity, leaves a little room for skepticism. We propose to explore the precise nature of this new phenomenon in future work.

Acknowledgments

One of us (P. A. THOMPSON) would like to acknowledge the support of the Research Corporation which made possible the first experimental test of this phenomenon, and the support of the Alexander von Humboldt Foundation which made possible the research reported here.

References

1. A. STODOLA, *Steam and gas turbines*, McGraw-Hill, New York 1927.
2. P. P. WEGENER, *Gas dynamics of expansion flows with condensation, and homogeneous nucleation of water vapor*, In Nonequilibrium Flows, vol. 1, Part 1 (ed. P.P. Wegener), Marcel Dekker, New York 1969.
3. P. A. THOMPSON, *Compressible-fluid dynamics*, p. 359, McGraw-Hill, New York 1972.
4. P. A. THOMPSON and D. A. SULLIVAN, *On the possibility of complete condensation shock waves in retrograde fluids*, J. Fluid Mech., 70, 639–650, 1975.
5. W. R. SMITH, *Vapor-liquid condensation in a shock tube*, In Recent Developments in Shock-Tube Research (Proc. Ninth Int. Shock Tube Symp.), Stanford Univ. Press, 1973.
6. L. DAVIES and J. L. WILSON, *The influence of shock and boundary layer interaction on shock tube flows*, In Proc. Sixth Int. Shock Tube Symp. Ernst-Mach-Institut, Freiburg i.B., 1968.

MAX-PLANCK-INSTITUT
FÜR STRÖMUNGSFORSCHUNG GÖTTINGEN.

Received October 22, 1975.